Quasielastic neutron scattering study of hydrogen motion in A15-type Nb_3AlH_x

A. V. Skripov[1] and L. S. Voyevodina[1]
[1]*Institute of Metal Physics, Urals Branch of the Academy of Sciences, Ekaterinburg 620219, Russia*

R. Hempelmann[2]
[2]*Institut für Physikalische Chemie, Universität des Saarlandes, D-66041 Saarbrücken, Germany*
(Received 6 September 2005; revised manuscript received 22 November 2005; published 12 January 2006)

In order to study the mechanism and parameters of hydrogen diffusion in A15-type intermetallic Nb_3Al, we have performed high-resolution quasielastic neutron scattering measurements in Nb_3AlH_x ($x=0.13$ and 1.77) over the temperature range 10–407 K. The experimental results are consistent with a coexistence of two hydrogen jump processes: the fast H motion along the chains formed by interstitial *d* (Nb_4) sites and the slower H jumps from one chain to another. It is found that the modified Chudley–Elliott model taking into account the structure of the *d*-site sublattice gives a qualitative description of the experimental data for $Nb_3AlH_{0.13}$. The faster jump process in $Nb_3AlH_{0.13}$ corresponding to the long-range H diffusion along the *d*-site chains is characterized by the activation energy of 194 meV. In $Nb_3AlH_{1.77}$ the *d*-site chains are more than half filled, and the faster jump process is well described in terms of a model of local H jumps within pairs of nearest-neighbor *d* sites on the chains.

DOI: 10.1103/PhysRevB.73.014302 PACS number(s): 66.30.Jt, 78.70.Nx

I. INTRODUCTION

The cubic intermetallic compounds A_3B with A15-type structure (space group $Pm\bar{3}n$) show a number of unusual physical properties.[1,2] Some of the A15-type compounds (mostly those with $A=$Ti and Nb) can absorb large amounts of hydrogen.[3–9] The host lattice usually retains the A15 structure after hydrogen absorption. Previous studies of the effects of hydrogen in A15 materials were devoted mainly to its impact on the superconducting transition temperature.[3–7,10] However, little is known about the hydrogen mobility and the mechanisms of H diffusion in these compounds. Nuclear magnetic resonance (NMR) studies of H mobility have been reported for the A15-type hydrides Ti_3IrH_x,[11] Ti_3SbH_x,[12] V_3GaH_x,[13] and Nb_3AlH_x.[14] While the results for Ti_3SbH_x, V_3GaH_x, and Nb_3AlH_x suggest complex diffusion mechanisms implying at least two frequency scales of H jumps,[12–14] the NMR data cannot give direct information on spatial aspects of hydrogen motion. Such information can be obtained from quasielastic neutron scattering (QENS) measurements probing both the temporal and spatial scales of atomic motion.[15,16] In the present work, we apply incoherent QENS to study the mechanism and parameters of H diffusion in the A15-type compound Nb_3Al. The Nb_3Al-H system appears to be particularly suitable for such a study since the incoherent scattering cross sections of both Nb and Al are very small.

X-ray diffraction studies[5] of Nb_3AlH_x at room temperature have shown that in the hydrogen concentration range $0.2 \leqslant x \leqslant 1.5$ there are two coexisting phases with the same A15-type host lattice, but with different lattice parameters. A single-phase state of Nb_3AlH_x with the A15-type host lattice has been found for $x<0.2$ and $1.5<x\leqslant 2.2$.[5] On the basis of the general trends of site occupancy in hydrides of intermetallic compounds[17] and the neutron diffraction data for A15-type $Nb_3SnH_{1.0}$,[4] $Ti_3SbD_{2.6}$,[18] Ti_3IrD_x,[19] and Nb_3AuH_x,[20] we may expect that H atoms in Nb_3AlH_x occupy the 6*d* positions of the space group $Pm\bar{3}n$ (i.e., the tetrahedral interstitial sites coordinated by four Nb atoms). This is also consistent with the neutron diffraction results for nonstoichiometric $Nb_3(Al_{0.84}Nb_{0.16})D_{2.52}$.[21] The unit cell of the A15-type lattice with interstitial *d* sites is shown in Fig. 1. *B* atoms form a bcc sublattice, and *A* atoms occupy the 6*c* sites (1/2, 1/4, 0) on the faces of the unit cell. The sublattice of *d* sites is isomorphous to that of *A* atoms. These sites form three sets of nonintersecting chains in the [100], [010], and [001] directions. The distance between the nearest-neighbor *d* sites in the chains, $r_1=a/2$, is 22% shorter than the shortest distance between *d* sites on different chains, $r_2=\sqrt{3}a/2\sqrt{2}$, where *a* is the lattice parameter. Since jump rates of hydrogen in intermetallics strongly depend on distances between the corre-

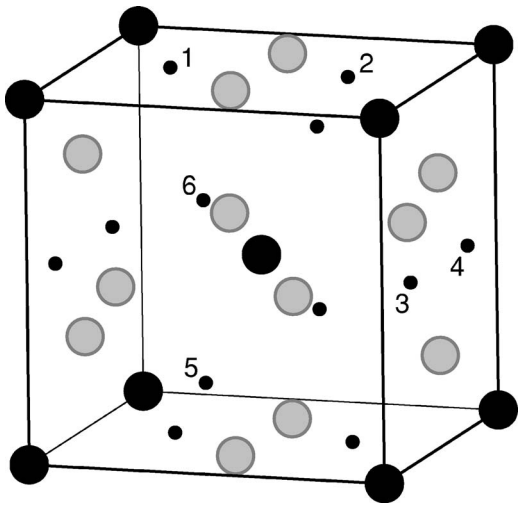

FIG. 1. The unit cell of A15-type compound A_3B with interstitial *d* sites. Large gray circles, *A* atoms; large black circles, *B* atoms; small black circles, *d* sites. The numbers correspond to six Bravais sublattices forming the lattice of *d* sites.

sponding sites,[22] a hydrogen atom is expected to perform many jumps along a chain before it jumps to another chain. Thus, the structure of the *d*-site sublattice in A15-type compounds suggests the possibility of quasi-one-dimensional effects on hydrogen diffusion.

II. THE JUMP MODEL

In this section we derive the incoherent dynamic structure factor for H diffusion over interstitial *d* sites in the A15-type lattice. We follow the approach of Ref. 23 generalizing the Chudley-Elliott model[24] to the case of non-Bravais lattices. In order to build a realistic jump model, in our case we have to take into account the jumps both to the nearest-neighbor and to the next-nearest-neighbor sites. The master equation for a diffusion process without correlations between consecutive steps can be written in terms of the conditional probability $P(\mathbf{r},t)$ of finding a particle on a site $\mathbf{r}$ at a time t if it was at the origin at $t=0$. The lattice of *d* sites in an A15-type structure consists of a superposition of six Bravais sublattices (Fig. 1) which are labeled by the subscripts m, n. We denote by $\mathbf{S}_{mn}^{\mathbf{k}}$ a jump vector from sublattice m to sublattice n with a distance vector of the elementary cells $\mathbf{k}$. For each of the six sublattices the master equation can be written as

$$\frac{\partial}{\partial t}P_n(\mathbf{r},t) = \sum_{m=1}^{6}\sum_{\mathbf{k}}\left[W_{mn}^{\mathbf{k}}P_m(\mathbf{r}+\mathbf{S}_{mn}^{\mathbf{k}},t) - W_{nm}^{\mathbf{k}}P_n(\mathbf{r},t)\right], \quad m \neq n, \tag{1}$$

where $W_{mn}^{\mathbf{k}}$ is the probability (per unit time) of a jump from sublattice m to sublattice n with the elementary cell vector $\mathbf{k}$. Each *d* site has two nearest neighbors (on the same chain) at the distance r_1 and eight next-nearest neighbors at the distance r_2. Therefore, in our model

$$W_{mn}^{\mathbf{k}} = \begin{cases} \dfrac{1}{2\tau_1} & \text{if the sites are separated by } r_1, \\ \dfrac{1}{8\tau_2} & \text{if the sites are separated by } r_2, \\ 0 & \text{otherwise.} \end{cases} \tag{2}$$

Here τ_1 and τ_2 are the mean residence times of a hydrogen atom at a site before a jump to one of the nearest and next-nearest sites, respectively.

The conditional probability densities for sublattices $P_n(\mathbf{r},t)$ are related to the self-correlation function $G_s(\mathbf{r},t)$ by

$$G_s(\mathbf{r},t) = \sum_{n=1}^{6} P_n(\mathbf{r},t), \tag{3}$$

which denotes the conditional probability density of finding a hydrogen atom at time t at position $\mathbf{r}$ (any sublattice) if it was at $t=0$ at the origin (any sublattice). The initial conditions are

$$G_s(\mathbf{r},0) = \delta(\mathbf{r}) \tag{4}$$

and

$$P_n(\mathbf{r},0) = \frac{1}{6}\delta(\mathbf{r}). \tag{5}$$

The Fourier transformation of $G_s(\mathbf{r},t)$ with respect to both space and time yields the incoherent dynamic structure factor $S_{inc}(\mathbf{Q},\omega)$ which is basically the quantity measured in QENS experiments.

The system of coupled equations (1) can be solved by Fourier transformation into momentum space

$$\frac{\partial}{\partial t}P_n(\mathbf{Q},t) = \sum_m P_m(\mathbf{Q},t)\left[\sum_{\mathbf{k}} W_{mn}^{\mathbf{k}}\exp(i\mathbf{Q}\mathbf{S}_{mn}^{\mathbf{k}}) - \delta_{mn}\sum_{l,\mathbf{k}} W_{nl}^{\mathbf{k}}\right], \tag{6}$$

where δ_{mn} is the Kronecker delta symbol. This system can be written as a matrix equation

$$\frac{\partial}{\partial t}\mathbf{P} = \tilde{\Lambda}\mathbf{P}, \tag{7}$$

where $\tilde{\Lambda}$ is the jump matrix with the elements

$$\tilde{\Lambda}_{nm} = \sum_{\mathbf{k}} W_{mn}^{\mathbf{k}}\exp(i\mathbf{Q}\mathbf{S}_{mn}^{\mathbf{k}}) - \delta_{mn}\sum_{l,\mathbf{k}} W_{nl}^{\mathbf{k}}. \tag{8}$$

Taking into account Eq. (2) and introducing the jump rate ratio $\alpha=\tau_1/\tau_2$, we obtain the jump matrix for our system in the form

$$\tilde{\Lambda} = \frac{1}{\tau_1}\begin{pmatrix} -(1+\alpha) & C_x & E_{xy}C_z & E_{xy}C_z & E_{xz}C_y & E_{xz}C_y \\ C_x & -(1+\alpha) & E_{xy}C_z & E_{xy}C_z & E_{xz}C_y & E_{xz}C_y \\ E_{xy}C_z & E_{xy}C_z & -(1+\alpha) & C_y & E_{yz}C_x & E_{yz}C_x \\ E_{xy}C_z & E_{xy}C_z & C_y & -(1+\alpha) & E_{yz}C_x & E_{yz}C_x \\ E_{xz}C_y & E_{xz}C_y & E_{yz}C_x & E_{yz}C_x & -(1+\alpha) & C_z \\ E_{xz}C_y & E_{xz}C_y & E_{yz}C_x & E_{yz}C_x & C_z & -(1+\alpha) \end{pmatrix} \tag{9}$$

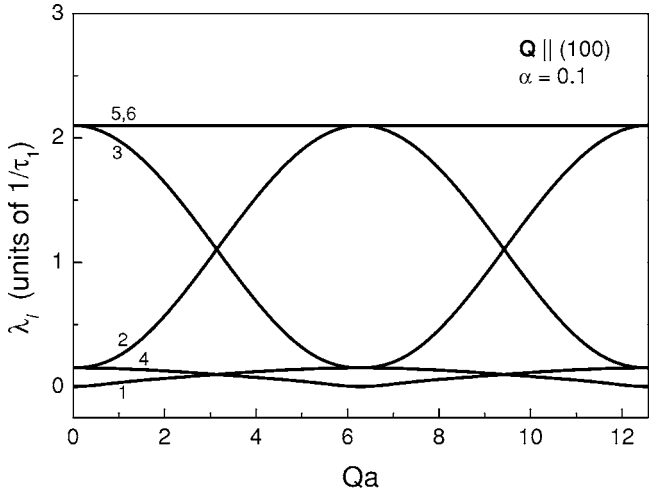

FIG. 2. The half-widths of six Lorentzian components resulting from the jump model with $\alpha = 0.1$ and $\mathbf{Q}\|[100]$ as functions of Qa.

where, for example, $C_x=\cos(aQ_x/2)$ and $E_{x\bar{y}}=(\alpha/4)\exp[ia(Q_x-Q_y)/4]$. Since $E^*_{x\bar{y}}=E_{\bar{x}y}$, this matrix is Hermitian. Following the standard procedures described in Ref. 23, we obtain the incoherent structure factor as a superposition of six Lorentzian lines,

$$S_{inc}(\mathbf{Q},\omega)=\frac{1}{\pi}\sum_{l=1}^{6} w_l \frac{-\lambda_l}{\lambda_l^2+\omega^2}, \tag{10}$$

where λ_l is an eigenvalue of the jump matrix, and

$$w_l=\frac{1}{6}\left|\sum_{n=1}^{6} v_l^n\right|^2, \tag{11}$$

v_l^n being the nth component of the eigenvector related to the eigenvalue λ_l.

The jump matrix can be diagonalized numerically for a given scattering vector $\mathbf{Q}$ and a given value of α. As an example of the results, Figs. 2 and 3 show the widths and relative intensities (weights) of six Lorentzian lines as functions of Qa for $\alpha=0.1$ and $\mathbf{Q}\|[100]$. For this direction of $\mathbf{Q}$, only two components (denoted as 1 and 2) have nonzero weights. At $Q\to 0$, there is only one diffusive mode with nonvanishing weight and the width proportional to Q^2; this is true for all directions of $\mathbf{Q}$. The weight of the broader component increases with increasing Q.

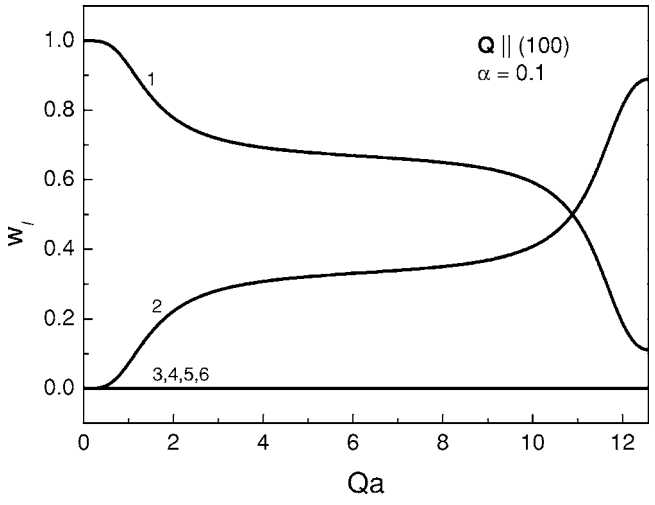

FIG. 3. The weights of six Lorentzian components resulting from the jump model with $\alpha = 0.1$ and $\mathbf{Q}\|[100]$ as functions of Qa.

III. EXPERIMENTAL DETAILS

The measurements were made on powdered samples of $Nb_3AlH_{0.13}$ and $Nb_3AlH_{1.77}$. The preparation of these samples has been described in Ref. 14. According to x-ray diffraction analysis, both $Nb_3AlH_{0.13}$ and $Nb_3AlH_{1.77}$ are single-phase compounds having the A15-type host-metal structure with the lattice parameters $a=5.190$ and 5.353 Å, respectively.

QENS spectra were measured on the high-resolution backscattering spectrometer IN16 at the Institute Laue-Langevin (ILL) in Grenoble. This spectrometer uses a Si(111) monochromator and analyzers selecting the neutron wavelength $\lambda=6.27$ Å. The range of energy transfer $\hbar\omega$ in our experiments was ± 14.3 μeV, the energy resolution being about 1.0 μeV (full width at half maximum). The range of momentum transfer $\hbar Q$ corresponded to a Q range of 0.43–1.93 Å^{-1}. The scattered neutrons were registered by two ^{3}He counters and the multidetector array (20 counters). The samples were placed into flat Al containers, the sample thickness being 1 mm for $Nb_3AlH_{0.13}$ and 0.3 mm for $Nb_3AlH_{1.77}$. The sample thickness was chosen to minimize the multiple-scattering effects; the neutron transmission coefficients calculated for $\lambda=6.27$ Å are 0.94 for $Nb_3AlH_{0.13}$ and 0.93 for $Nb_3AlH_{1.77}$. The planes of the containers were oriented in the direction of the only Bragg reflection ($2\theta\approx 108^\circ$) in the Q range studied. For each of the samples QENS spectra were recorded at seven temperatures in the ranges 10–407 K ($Nb_3AlH_{0.13}$) and 10–394 K ($Nb_3AlH_{1.77}$). In order to improve the statistics, some of the detectors were grouped in pairs. The raw experimental data were corrected for absorption and self-shielding using the standard ILL programs. The instrumental resolution functions were determined from the measured QENS spectra of Nb_3AlH_x at 10 K. The background spectra were measured for the empty sample containers in the same experimental geometry as for Nb_3AlH_x.

IV. RESULTS AND DISCUSSION

For both samples a quasielastic broadening of the neutron spectra has been observed at temperatures above 290 K. The experimental QENS spectra at $T>290$ K can be satisfactorily described by a sum of two components: the elastic line represented by the instrumental resolution function $R(Q,\omega)$ and the resolution-broadened Lorentzian quasielastic line. As an example of the data, Fig. 4 shows the QENS spectrum of $Nb_3AlH_{1.77}$ recorded at 360 K for $Q=1.53$ Å^{-1}. We have fitted the experimental scattering function $S_{expt}(Q,\omega)$ with the model incoherent scattering function

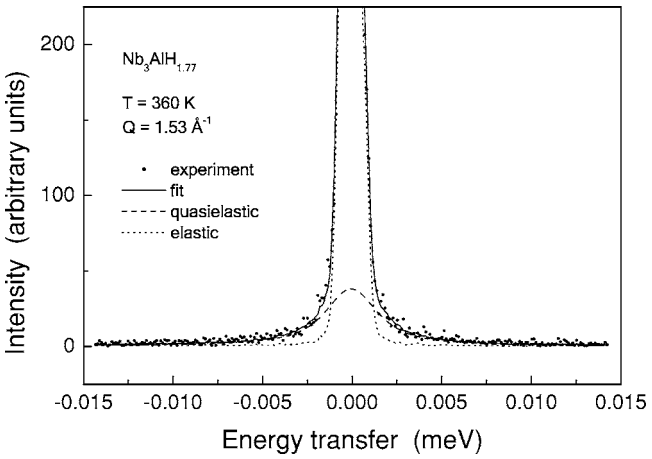

FIG. 4. The QENS spectrum for $Nb_3AlH_{1.77}$ measured on IN16 at $T=360$ K and $Q=1.53$ Å^{-1}. The solid curve shows the fit of the two-component model [Eq. (12)] to the data. The dotted curve represents the spectrometer resolution function (the elastic component), and the dashed curve shows the Lorentzian quasielastic component.

$$S_{\mathrm{inc}}(Q,\omega) = A_0(Q)\delta(\omega) + [1 - A_0(Q)]L(\omega,\Gamma) \qquad (12)$$

convoluted with $R(Q,\omega)$. Here $\delta(\omega)$ is the elastic delta function, $L(\omega,\Gamma)$ is the quasielastic Lorentzian with the half-width Γ, and $A_0(Q)$ is the elastic incoherent structure factor (EISF). The width of the quasielastic component is found to increase with increasing temperature. Figure 5 shows the behavior of Γ as a function of the inverse temperature. It can be seen that for both samples the temperature dependence of Γ is well described by the Arrhenius relation; the corresponding activation energies are 194 ± 17 meV for $Nb_3AlH_{0.13}$ and 163 ± 16 meV for $Nb_3AlH_{1.77}$.

Figure 6 shows the Q dependence of the half-width of the quasielastic component for $Nb_3AlH_{0.13}$ ($T=374$ K) and $Nb_3AlH_{1.77}$ ($T=360$ K). As can be seen from this figure,

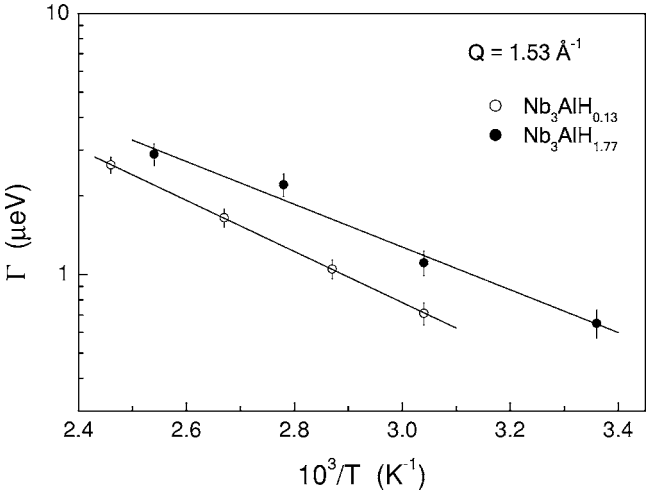

FIG. 5. The half-widths of the quasielastic lines for $Nb_3AlH_{0.13}$ and $Nb_3AlH_{1.77}$ at $Q=1.53$ Å^{-1} as functions of the inverse temperature. The solid lines show the Arrhenius fits to the data.

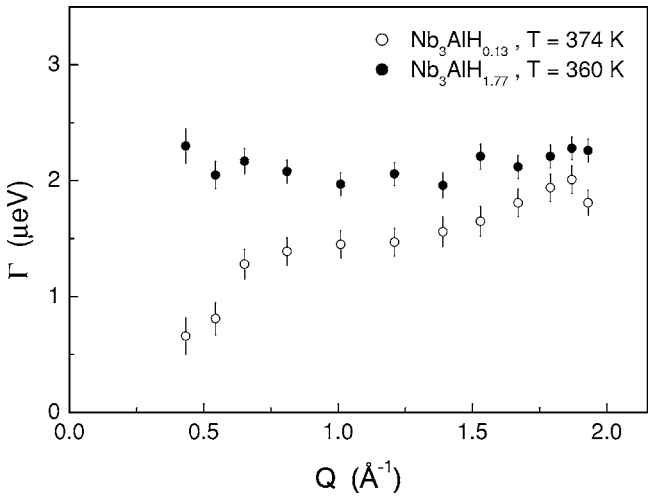

FIG. 6. The half-widths of the quasielastic lines for $Nb_3AlH_{0.13}$ ($T=374$ K) and $Nb_3AlH_{1.77}$ ($T=360$ K) as functions of Q.

there is a strong difference between the Q dependences of Γ for the samples with high ($x=1.77$) and low ($x=0.13$) hydrogen concentrations. It should be noted that for each of the samples the Q dependence of Γ remains qualitatively unchanged in the temperature range 290–407 K. For $Nb_3AlH_{1.77}$ the half-width of the quasielastic line appears to be nearly Q independent. Such a behavior is typical of the case of spatially confined (localized) motion.[15,16] It is natural to assume that for $Nb_3AlH_{1.77}$ the faster jump process (which, in the temperature range studied, is probed by the backscattering spectrometer) is associated with back-and-forth jumps of H atoms within pairs of the nearest-neighbor d sites along the chains. In fact, since the complete filling of d sites corresponds to $x=3$, for $x=1.77$ the chains of d sites are more than half filled. Therefore, the fast long-range diffusion along the chains should be suppressed, so that the dominant type of fast H motion is likely to be represented by localized jumps of hydrogen atoms between the nearest-neighbor sites. In order to verify this, we have to consider the Q dependence of the EISF shown in Fig. 7. In the case of local jumps within pairs of sites separated by a distance l, the orientationally averaged expression for the EISF can be written in the form[15,16]

$$A_0(Q) = 1 - p + \frac{p}{2}[1 + j_0(Ql)], \qquad (13)$$

where $j_0(x)$ is the sperical Bessel function of zeroth order and p is the fraction of H atoms participating in the localized motion. The values of p may be less than 1, since for concentrated hydrides some H atoms at d sites may be blocked due to occupation of both nearest-neighbor sites on the chain by other H atoms. The existence of a temperature-dependent fraction of H atoms not participating in the fast localized motion has been observed in a number of metal-hydrogen systems;[25–29] it has been attributed to the effects of H-H interactions.[25,26] As noted in Ref. 30, Eq. (13) with $4\rho/(1+\rho)^2$ substituted for p also describes the Q dependence of the EISF for the model of local jumps in an asymmetric

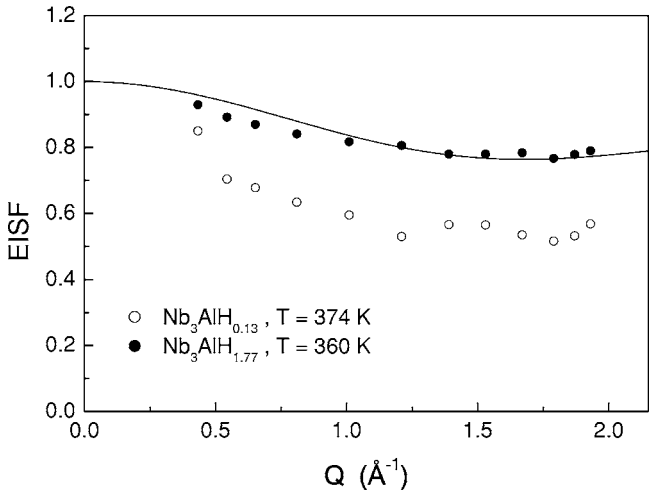

FIG. 7. The elastic incoherent structure factors for $Nb_3AlH_{0.13}$ (T=374 K) and $Nb_3AlH_{1.77}$ (T=360 K) as functions of Q. The solid line shows the fit of the two-site model [Eq. (13)] with the fixed l=2.68 Å to the data for $Nb_3AlH_{1.77}$.

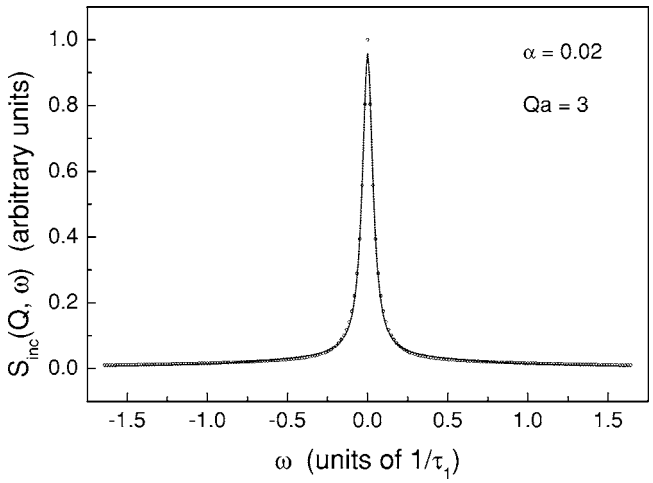

FIG. 8. The orientationally averaged model QENS spectrum for α=0.02 and Qa=3. The dashed curve shows the fit of this model spectrum with a sum of two Lorentzians.

double-well potential, where ρ is the ratio of back-and-forth jump rates. Therefore, on the basis of experimental $A_0(Q)$ data it is impossible to distinguish between the model of two-site motion in a symmetric double-well potential with a fraction of "static" atoms ($p \neq 1$) and the model of two-site motion in an asymmetric potential ($\rho \neq 1$). The period of the oscillating Q dependence described by Eq. (13) is determined by the jump length l. In order to compare the Q dependence of the EISF predicted by this equation with our experimental data for $Nb_3AlH_{1.77}$, we can fix l to the value of the actual distance between the nearest-neighbor d sites on the chains, $r_1=a/2=2.68$ Å, so that p is the only fit parameter. The solid line in Fig. 7 shows the fit of Eq. (13) with the fixed l=2.68 Å to the data for $Nb_3AlH_{1.77}$; the corresponding value of p is 0.39±0.02. It can be seen that the experimental $A_0(Q)$ dependence for $Nb_3AlH_{1.77}$ is consistent with the model of localized H motion within pairs of the nearest-neighbor d sites on the chains. Similar results are obtained at other temperatures in the range 298–394 K, the value of p showing a certain increase with increasing T.

For $Nb_3AlH_{0.13}$ the half-width of the quasielastic line increases with increasing Q (see Fig. 6). It is evident that the model implying a dominant role of localized H motion is not applicable for the sample with low hydrogen concentration. We can assume that H jumps in $Nb_3AlH_{0.13}$ are not correlated; therefore, the modified Chudley-Elliott model discussed in Sec. II may be applicable. In order to compare the results of the model calculations with the experimental data for the powdered sample, it is necessary to average the numerical results over all directions of the **Q** vector. The ratio of the jump rates $\alpha=\tau_1/\tau_2$ has been fixed to 0.02. Taking into account the ratios of H jump rates in other intermetallics,[22] this value seems to be reasonable for $r_2/r_1=1.22$. The orientational averaging of the model has been made in the following way. For a certain length of the **Q** vector, $Q=|\mathbf{Q}|$, and for all possible pairs of angles (θ,φ) defining the direction of **Q**, the jump matrix (9) is diagonalized numerically, and the derived QENS spectra (10) are summed with the weight factor of sin θ. This procedure yields the orientationally averaged model spectrum $S_{\mathrm{inc}}(Q,\omega)$. As examples of the results, Figs. 8 and 9 show the shapes of the model spectra for Qa=3 and 10, respectively. Note that these two spectra have different scales of the energy transfer. All the orientationally averaged model spectra look like a superposition of two lines with different widths. This feature could be expected, since our jump model implies two frequency scales of H motion. It should be noted that the shape of the narrow component may also be affected by the divergency of the powder averaged $S_{\mathrm{inc}}(Q,\omega)$ at ω=0 for the case of one-dimensional diffusion.[31]

The experimental QENS spectra have been described in terms of Eq. (12); therefore, for parametrization of the model spectra it would be natural to use a sum of two Lorentzian lines. The fits of the model spectra with a sum of two Lorentzian lines appear to be reasonable for all values of Q; the fits for Qa=3 and 10 are shown by dashed curves in Figs. 8 and 9. We may assume that the narrow component of the model

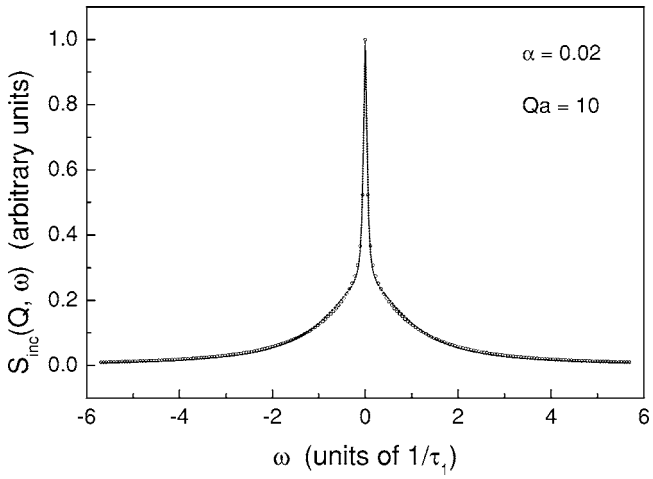

FIG. 9. The orientationally averaged model QENS spectrum for α=0.02 and Qa=10. The dashed curve shows the fit of this model spectrum with a sum of two Lorentzians.

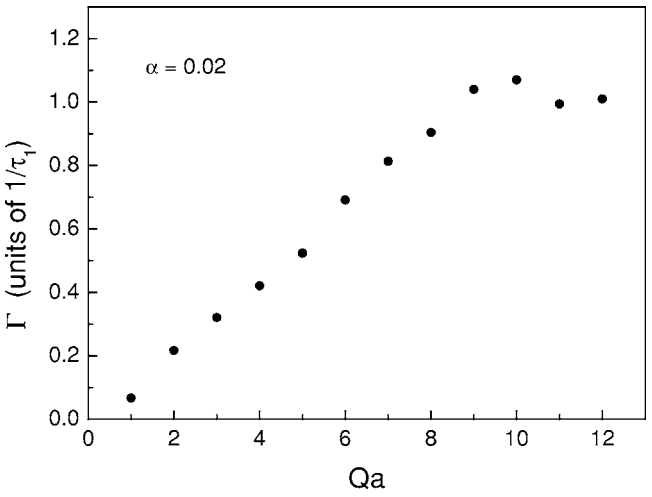

FIG. 10. The half-width of the broader Lorentzian component (resulting from the two-component fits of the model QENS spectra for $\alpha=0.02$) as a function of Qa.

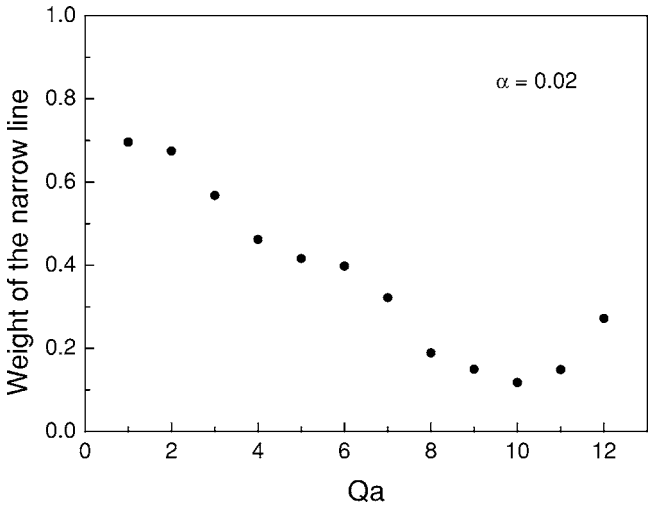

FIG. 11. The relative intensity of the narrow Lorentzian component (resulting from the two-component fits of the model QENS spectra for $\alpha=0.02$) as a function of Qa.

spectra corresponds to the "elastic" line of the experimental spectra for $Nb_3AlH_{0.13}$. This means that the width of the narrow component is too small to be resolved in the studied temperature range. Therefore, we have to consider the Q dependences of the width of the broad component and the relative intensity of the narrow component of the model spectra. These Q dependences resulting from the two-component fits of the model spectra are shown in Figs. 10 and 11. It should be noted that these Q dependences remain practically the same over a wide range of the jump rate ratio α. In fact, our model calculations using $\alpha=0.002$ and 0.01 result in Q dependences of the width of the broad component (in units of τ_1^{-1}) and a relative intensity of the narrow component which nearly coincide with those shown in Figs. 10 and 11. For the case of $\alpha=0$ corresponding to strictly one-dimensional diffusion, the narrow component is determined by the divergency of $S_{\mathrm{inc}}(Q,\omega)$ mentioned above. In this case the description of the model spectra by a sum of two Lorentzians is worse than for $\alpha=0.02$; however, the resulting Q dependences of the width of the broad component (in units of τ_1^{-1}) and the relative intensity of the narrow component are still close to those shown in Figs. 10 and 11.

In order to compare these Q dependences with the experimental data for $Nb_3AlH_{0.13}$ (Figs. 6 and 7), we have to take into account that the lowest experimental value of Q (0.43 $\mathrm{Å}^{-1}$) corresponds to $Qa\approx 2.2$, and the highest experimental value of Q (1.93 $\mathrm{Å}^{-1}$) corresponds to $Qa\approx 10$. It can be seen that the model qualitatively describes the behavior of the QENS data for $Nb_3AlH_{0.13}$: the increase in the quasielastic linewidth as a function of Q with the signs of saturation at the high-Q end, and the decrease in the elastic line intensity with the signs of saturation at the high-Q end. However, the drop in the relative intensity of the elastic line resulting from the model calculations (Fig. 11) is considerably stronger than the experimental one for $Nb_3AlH_{0.13}$ (Fig. 7). A similar feature has been found[32,33] for cubic Laves phases, where H jump motion shows two frequency scales: the relative intensity of the elastic line resulting from the Monte Carlo simulation of the QENS spectra falls down to considerably lower values than the experimental EISF. Such a discrepancy presumably originates from the fact that the interaction between H atoms is not taken into account in the model calculations.

Using the results of the model calculations, we can estimate the hydrogen jump rates τ_1^{-1}. For example, it follows from Fig. 10 that at $Q=1.53$ $\mathrm{Å}^{-1}$ (corresponding to $Qa\approx 8$ for $Nb_3AlH_{0.13}$) the half-width of the broad component is approximately $0.9\hbar\,\tau_1^{-1}$. Thus, it is possible to transform the temperature dependence of Γ shown in Fig. 5 into the temperature dependence of τ_1^{-1}. For $Nb_3AlH_{0.13}$ this approach leads to Arrhenius-type behavior of $\tau_1^{-1}(T)$ with the activation energy $E_a=194\pm 17$ meV and the preexponential factor $\tau_{10}^{-1}=(1.1\pm 0.6)\times 10^{12}$ s^{-1}. For the localized two-site motion, the relation between the jump rate and the half-width of the quasielastic line is given by $\Gamma=2\hbar\,\tau_1^{-1}$.[15,16] Hence, for $Nb_3AlH_{1.77}$ the behavior of $\tau_1^{-1}(T)$ can be described by an Arrhenius-type dependence with the activation energy $E_a=163\pm 16$ meV and the preexponential factor $\tau_{10}^{-1}=(2.7\pm 1.4)\times 10^{11}$ s^{-1}. The resulting Arrhenius plots of $\tau_1^{-1}(T)$ for $Nb_3AlH_{0.13}$ and $Nb_3AlH_{1.77}$ are shown in Fig. 12 by the solid and dashed lines, respectively. Note that while the measured values of Γ for $Nb_3AlH_{0.13}$ are lower than for $Nb_3AlH_{1.77}$ (Fig. 5), the hydrogen jump rates τ_1^{-1} for $Nb_3AlH_{0.13}$ appear to be higher than those for $Nb_3AlH_{1.77}$ in the range 290–400 K.

The present QENS measurements do not give any direct information on the slower hydrogen jump process, since the corresponding jump rates in the studied T range are too low to be resolved by the backscattering neutron spectrometer. Because of a possible hydrogen desorption, measurements at $T>420$ K have not been performed. However, it is interesting to compare the present QENS results with the NMR measurements of the proton spin-lattice relaxation rate R_1 for the same Nb_3AlH_x samples,[14] since the NMR measurements are usually sensitive to lower jump rates than the backscattering QENS measurements. The characteristic feature of the proton spin-lattice relaxation data in metal-hydrogen systems is the $R_1(T)$ maximum observed at the temperature at

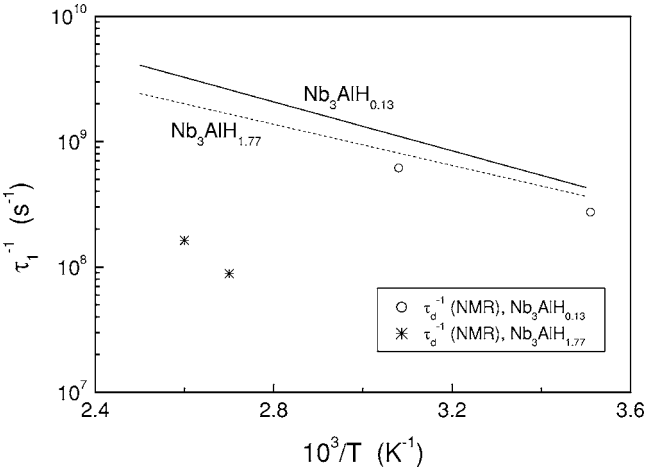

FIG. 12. The temperature dependences of the hydrogen jump rates for the faster jump process, as derived from the QENS data for $Nb_3AlH_{0.13}$ (solid line) and $Nb_3AlH_{1.77}$ (dashed line). The circles and stars represent the H jump rates estimated from the maxima of the proton spin-lattice relaxation rates for the same samples.

which $\omega_0\tau_d \approx 1$, where $\omega_0/2\pi$ is the NMR frequency and τ_d is the correlation time for the dipole-dipole interaction between nuclear spins.[34] For Nb_3AlH_x the proton spin-lattice relaxation rate is dominated by ^{1}H-^{93}Nb dipole-dipole interactions,[14] and τ_d^{-1} can be identified as an appropriate H jump rate. The values of τ_d^{-1} at the R_1 maxima have been estimated from the condition $\omega_0\tau_d=0.92$ corresponding to the Bloembergen-Purcell-Pound (BPP) model.[35] For $Nb_3AlH_{1.77}$ the R_1 maximum is observed at 370 K for $\omega_0/2\pi=13$ MHz and at 384 K for $\omega_0/2\pi=23.8$ MHz;[14] the corresponding values of τ_d^{-1} are shown by stars in Fig. 12. It can be seen that for $Nb_3AlH_{1.77}$ the H jump rates τ_d^{-1} evaluated from the NMR data are considerably lower than the jump rates τ_1^{-1} in the same temperature range. Thus, it is natural to assume that the R_1 maximum for $Nb_3AlH_{1.77}$ is determined by the slower H jump process leading to long-range diffusion. Such a situation is typical for those metal-hydrogen systems where a long-range H diffusion coexists with the faster localized H motion:[22,36] the main R_1 peak is determined by the long-range diffusion, while the localized motion either contributes to the low-temperature slope of this peak or gives rise to a secondary R_1 peak at low T. Identifying τ_d^{-1} with τ_2^{-1}, we obtain the H jump ratio $\alpha=0.05$ for $Nb_3AlH_{1.77}$ at 370 K. Because of the difference between the activation energies of the two hydrogen jump processes,[22,36] this ratio usually decreases with decreasing temperature.

For $Nb_3AlH_{0.13}$ the R_1 maximum is observed at 285 K for $\omega_0/2\pi=40$ MHz and at 325 K for $\omega_0/2\pi=90$ MHz;[14] the corresponding values of τ_d^{-1} are shown by circles in Fig. 12. In contrast to the case of $Nb_3AlH_{1.77}$, these values of τ_d^{-1} appear to be close to the $\tau_1^{-1}(T)$ line for $Nb_3AlH_{0.13}$. Moreover, the analysis of the $R_1(T)$ data for $Nb_3AlH_{0.13}$ in terms of the BPP model with a Gaussian distribution of activation energies gives the preexponential factor $\tau_{d0}^{-1}=1.25\times10^{12}$ s^{-1} and the average activation energy $E_a^d=210$ meV.[14] The values of these parameters are close to the corresponding values for $\tau_1^{-1}(T)$ in $Nb_3AlH_{0.13}$ (see above). Therefore, we can conclude that the observed R_1 peak in $Nb_3AlH_{0.13}$ is determined by the same fast H jump process which is responsible for the broad component in the QENS spectra. The effects of the slower H jump process are presumably hidden on the high-temperature slope of the $R_1(T)$ peak. The difference between the nature of the $R_1(T)$ data in the dilute and concentrated hydrides may be ascribed to the fact that, in contrast to the case of $Nb_3AlH_{1.77}$, the faster jump process in $Nb_3AlH_{0.13}$ corresponds to *long-range* motion.

V. CONCLUSIONS

The analysis of our QENS data for A15-type Nb_3AlH_x ($x=0.13$ and 1.77) suggests that in both samples there are at least two H jump processes with different characteristic frequencies. Although in both samples H atoms randomly occupy sites of the same type (d sites forming three sets of chains), the microscopic picture of H motion in the sample with high hydrogen concentration differs from that in the sample with low hydrogen concentration.

For $Nb_3AlH_{1.77}$ the faster jump process is well described in terms of the model of *local* H jumps within pairs of the nearest-neighbor d sites on the chains. In the temperature range 298–394 K the H jump rate τ_1^{-1} of the faster process shows Arrhenius-type behavior with the activation energy $E_a=163\pm16$ meV and the preexponential factor $\tau_{10}^{-1}=(2.7\pm1.4)\times10^{11}$ s^{-1}. While the present QENS experiments cannot give any direct information on the slower jump process (corresponding to H jumps from one chain to another), this process has been probed by the NMR measurements.[14] The ratio of the jump rates for the two processes estimated from the comparison of the NMR and QENS results for $Nb_3AlH_{1.77}$ is 0.05 at $T=370$ K.

For the case of low H concentrations in A15-type compounds we have found the solutions of the modified Chudley-Elliott model corresponding to the fast motion of H atoms along the d-site chains and the slower jumps from one chain to another. These solutions qualitatively describe the main features of our QENS data for $Nb_3AlH_{0.13}$. The comparison of the model calculations with the experimental QENS results for $Nb_3AlH_{0.13}$ shows that in the temperature range 329–407 K the hydrogen jump rate τ_1^{-1} of the faster process can be described by an Arrhenius law with the activation energy $E_a=194\pm17$ meV and the preexponential factor $\tau_{10}^{-1}=(1.1\pm0.6)\times10^{12}$ s^{-1}. Since in the case of $Nb_3AlH_{0.13}$ the faster jump process corresponds to long-range H diffusion along the chains, this process also gives the dominant contribution to the proton spin-lattice relaxation rate measured by NMR.

AKNOWLEDGMENTS

The authors are grateful to J. Combet for assistance with the quasielastic neutron scattering measurements at ILL and to A. Melyokhin for assistance with the model calculations. This work was supported by the Russian Foundation for Basic Research (Grant No. 03-02-16063) and by the Priority Program "Hydrogen Energy" of the Russian Academy of Sciences. A.V.S. also acknowledges financial support from Universität des Saarlandes.

[1] S. V. Vonsovsky, Yu. A. Izyumov, and E. Z. Kurmaev, *Superconductivity of Transition Metals, Their Alloys and Compounds* (Springer, Berlin, 1982).
[2] J. Muller, Rep. Prog. Phys. **43**, 641 (1980).
[3] P. R. Sahm, Phys. Lett. **26A**, 459 (1968).
[4] L. J. Vieland, A. W. Wicklund, and J. G. White, Phys. Rev. B **11**, 3311 (1975).
[5] V. F. Shamrai and L. N. Padurets, Dokl. Akad. Nauk SSSR **246**, 1182 (1979).
[6] S. Z. Huang, T. Skowskiewicz, C. W. Chu, and J. L. Smith, Phys. Rev. B **22**, 137 (1980).
[7] V. E. Antonov, T. E. Antonova, I. T. Belash, O. V. Zharikov, A. I. Latynin, A. V. Palnichenko, and V. I. Rashchupkin, Sov. Phys. Solid State **31**, 1659 (1989).
[8] M. Schlereth and H. Wipf, J. Phys.: Condens. Matter **2**, 6927 (1990).
[9] M. Baier, R. Wordel, F. E. Wagner, T. E. Antonova, and V. E. Antonov, J. Less-Common Met. **172**, 358 (1991).
[10] K. V. S. Rama Rao, H. Sturm, B. Elschner, and A. Weiss, Phys. Lett. **93A**, 492 (1983).
[11] D. Guthardt, D. Beisenherz, and H. Wipf, J. Phys.: Condens. Matter **4**, 6919 (1992).
[12] A. V. Skripov, M. Yu. Belyaev, and S. A. Petrova, J. Phys.: Condens. Matter **4**, L537 (1992).
[13] A. V. Skripov, Yu. G. Cherepanov, and H. Wipf, J. Alloys Compd. **209**, 111 (1994).
[14] A. V. Skripov, A. V. Soloninin, A. P. Stepanov, and V. N. Kozhanov, J. Phys.: Condens. Matter **12**, 9607 (2000).
[15] M. Bée, *Quasielastic Neutron Scattering* (Hilger, Bristol, 1988).
[16] R. Hempelmann, *Quasielastic Neutron Scattering and Solid State Diffusion* (Clarendon Press, Oxford, 2000).
[17] K. Yvon and P. Fischer, in *Hydrogen in Intermetallic Compounds I*, edited by L. Schlapbach (Springer, Berlin, 1988), p. 87.
[18] A. V. Skripov, A. A. Podlesnyak, and P. Fischer, J. Alloys Compd. **210**, 27 (1994).
[19] K. Cornell, H. Wipf, U. Stuhr, and A. V. Skripov, Solid State Commun. **101**, 569 (1997).
[20] V. E. Antonov, E. I. Bokhenkov, B. Dorner, V. K. Fedotov, G. Grosse, A. I. Latynin, F. E. Wagner, and R. Wordel, J. Alloys Compd. **264**, 1 (1998).
[21] Y. Andersson, T. Larsson, B. Nolang, and S. Rundqvist, J. Alloys Compd. **306**, 193 (2000).
[22] A. V. Skripov, Defect Diffus. Forum **224-225**, 75 (2003).
[23] J. M. Rowe, K. Sköld, H. E. Flotow, and J. J. Rush, J. Phys. Chem. Solids **32**, 41 (1971).
[24] C. T. Chudley and R. J. Elliott, Proc. Phys. Soc. London **77**, 353 (1961).
[25] N. F. Berk, J. J. Rush, T. J. Udovic, and I. S. Anderson, J. Less-Common Met. **172**, 496 (1991).
[26] A. V. Skripov, J. C. Cook, D. S. Sibirtsev, C. Karmonik, and R. Hempelmann, J. Phys.: Condens. Matter **10**, 1787 (1998).
[27] A. V. Skripov, M. Pionke, O. Randl, and R. Hempelmann, J. Phys.: Condens. Matter **11**, 1489 (1999).
[28] A. V. Skripov, J. C. Cook, C. Karmonik, and V. N. Kozhanov, Phys. Rev. B **60**, 7238 (1999).
[29] E. Mamontov, T. J. Udovic, O. Isnard, and J. J. Rush, Phys. Rev. B **70**, 214305 (2004).
[30] A. V. Skripov, J. C. Cook, C. Karmonik, and R. Hempelmann, J. Phys.: Condens. Matter **8**, L319 (1996).
[31] K. Hahn, H. Jobic, and J. Kärger, Phys. Rev. E **59**, 6662 (1999).
[32] D. J. Bull, Ph.D. thesis, University of Salford, 2001.
[33] D. J. Bull, D. P. Broom, and D. K. Ross, Chem. Phys. **292**, 153 (2003).
[34] R. G. Barnes, in *Hydrogen in Metals III*, edited by H. Wipf (Springer, Berlin, 1997), p. 93.
[35] N. Bloembergen, E. M. Purcell, and R. M. Pound, Phys. Rev. **73**, 679 (1948).
[36] A. V. Skripov, A. V. Soloninin, A. L. Buzlukov, L. S. Voyevodina, J. C. Cook, T. J. Udovic, and R. Hempelmann, J. Phys.: Condens. Matter **17**, 5011 (2005).